Nanoscale

PAPER

View Article Online
View Journal | View Issue

Cite this: *Nanoscale*, 2023, **15**, 16984

Efficient and reliable encapsulation for perovskite/silicon tandem solar modules†

Francesco Toniolo,‡[a,b] Helen Bristow,[a] Maxime Babics,[a] Livia M. D. Loiola,[c] Jiang Liu,[a] Ahmed Ali Said,[a] Lujia Xu,[a] Erkan Aydin,[a] Thomas G. Allen,[a] Moreno Meneghetti,[b] Suzana P. Nunes,[c] Michele De Bastiani*‡[a] and Stefaan De Wolf*[a]

Perovskite/silicon tandem solar cells have a tremendous potential to boost renewable electricity production thanks to their very high performance combined with promising cost structure. However, for actual field deployment, any solar cell technology needs to be assembled into modules, where the associated processes involve several challenges that may affect both the performance and stability of the devices. For instance, due to its hygroscopic nature, ethylene vinyl acetate (EVA) is incompatible with perovskite-based photovoltaics. To circumvent this issue, we investigate here two alternative encapsulant polymers for the packaging of perovskite/silicon tandems into minimodules: a thermoplastic polyurethane (TPU) and a thermoplastic polyolefin (TPO) elastomer. To gauge their impact on tandem-module performance and stability, we performed two internationally established accelerated module stability tests (IEC 61215): damp heat exposure and thermal cycling. Finally, to better understand the thermomechanical properties of the two encapsulants and gain insight into their relation to the thermal cycling of encapsulated tandems, we performed a dynamic mechanical thermal analysis. Our understanding of the packaging process of the tandem module provides useful insights for the development of commercially viable perovskite photovoltaics.

Received 8th December 2022,
Accepted 14th September 2023

DOI: 10.1039/d2nr06873g

rsc.li/nanoscale

Introduction

Over the last fifteen years, metal halide perovskite solar cells (PSCs) have gathered tremendous interest as a potentially disruptive photovoltaic (PV) technology. Thanks to their excellent optoelectronic properties such as a steep absorption edge,[1] defect tolerance,[2] and tunable bandgap,[3] combined with sophistication of device processing, PSCs have achieved power conversion efficiencies (PCEs) close to 26% in their single-junction implementation and more than 33% for perovskite/silicon tandem configurations.[4,5] However, despite this remarkable progress in performance, perovskite PV is still pestered by a lack of long-term stability, which poses currently the largest roadblock towards commercialization.[6] To reach market maturity, PV modules composed of PSCs must meet relevant established international standards of certification, such as IEC 61215; the passing of additional, perovskite-specific tests may be required too.[7] To fulfil this challenge, significant efforts have already been undertaken to improve the stability of PSCs at the materials and device levels. Early attempts aimed at tailoring the perovskite formulations,[8] to improve the resilience of PSCs to light and temperature exposure.[9] Subsequently, interface modifications of the perovskite photo-absorber, such as those based on two-dimensional (2D) perovskite approaches, were found to further improve device stability.[10] Recently, we also witnessed excellent progress in the development of appropriate encapsulation processes for PSCs, resulting in the first prototypes of perovskite solar modules.[11] In this, besides offering mechanical robustness, the main purpose of encapsulation is to protect the perovskite absorber from harmful environmental stressors, such as moisture and oxygen, which often are found to be major causes of immediate, irreversible degradation of the device.[12–14]

[a]*KAUST Solar Center (KSC), Physical Sciences and Engineering Division (PSE), King Abdullah University of Science and Technology (KAUST), Thuwal 23955-6900, Kingdom of Saudi Arabia. E-mail: stefaan.dewolf@kaust.edu.sa, michele.debastiani@kaust.edu.sa*

[b]*Department of Chemical Science, Università degli Studi di Padova, Via F. Marzolo 1, 35131 Padova, Italy*

[c]*Nanostructured Polymer Membrane Laboratory, Biological and Environmental Science and Engineering Division (BESE), King Abdullah University of Science and Technology (KAUST), Thuwal, 23955-6900, Saudi Arabia*

†Electronic supplementary information (ESI) available. See DOI: https://doi.org/10.1039/d2nr06873g

‡Current affiliation: Department of Chemistry & INSTM Università di Pavia, Via T. Taramelli 14, Pavia 27100, Italy.

Technological evolution of perovskite solar minimodules

Historically, the first encapsulation approach for PSCs consisted in embedding the device in epoxy resins.[15] However, these resins form only a weak barrier against moisture and oxygen ingress over prolonged exposure, making them unsuitable for accelerated testing or long-term outdoor deployment (which should be aimed at >25 years of operational lifetime). The second generation of encapsulation sandwiched PSCs between two pieces of glass sheets without polymeric lamination sheets, but using butyl rubber as edge sealant.[16] This approach enabled the first successful passing of the accelerated stability test (IEC 61215, damp heat, and humidity freeze) for single-junction PSCs.[11] However, it was soon found that the byproducts generated during the tests may accelerate device degradation.[11] Moreover, this approach is not ideal for the encapsulation of perovskite/silicon tandem devices, due to the notable optical losses stemming from the air gap between the front glass and the device.[17] The third generation of PSCs encapsulation saw the first attempt at vacuum lamination, which is the traditional method used in the PV industry (both by wafer-based crystalline-silicon (c-Si) and thin-film PV manufacturers) to seal the modules. For wafer-based PV, in vacuum lamination, the devices are sandwiched between a front and rear protection sheet (glass at the front, either glass or a polymeric sheet at the back) and a polymeric lamination sheet on both device sides. Meanwhile, thin-film devices are usually commercialized in the glass superstrate configuration, where only at the back side lamination needs to be applied. In either implementation, during the lamination process, the polymeric encapsulant melts during heating and solidifies during subsequent cooling.[18] Thin-film technologies such as CIGS, micromorph and amorphous silicon often employed ethylene vinyl acetate (EVA) as an encapsulant in most commercial products, in the form of medium and large-area modules. For CdTe modules, thermoplastic polyolefin (TPO) is mainly used, rarely EVA. This is due to the higher voltage output of the modules and the higher resilience of TPO to potential induced degradation (PID). Alternatives, even if expensive, based on multi-layer architectures were also considered at the R&D level with remarkable stability results.[19] For CIGS modules, it was demonstrated that EVA could cause problematic compressive stress in the device during the lamination. This effect was correlated to the percentage of gel of the EVA and the amount of cross-linker.[20] Similarly to CdTe, even for CIGS, alternative encapsulation processes based on multi-layer, conformal oxides *via* atomic layer deposition were found to be successful. For micromorph and amorphous silicon modules in rigid configuration, EVA and polyisobutylene were the most common encapsulants; alternative encapsulants for flexible applications were not proven stable.

Similarly to CIGS technology, EVA is not suitable for perovskite module PV, as it requires a lamination temperature >140 °C, which is harmful to the perovskite.[21–23] Moreover, the cross-linking process (complete or partial) of the EVA encapsulant releases acidic byproducts that degrade the perovskite.[24,25] Therefore, identifying alternative encapsulants to EVA represents a critical step forward toward the realization of stable perovskite PV, closing the gap with commercialization. In this direction, thermoplastic polyolefin (TPO) elastomer is a potential candidate. In addition, for perovskite PV, it is advisable to also use a glass protection sheet at the rear side to avoid moisture ingress.

In this work, we fabricated wafer-based perovskite/silicon tandem minimodules by sandwiching tandem devices between two glass sheets, using two different thermoplastic elastomeric encapsulants, a thermoplastic polyurethane (TPU) and a commercial polyolefin-based encapsulant (TPO). We investigated the minimodules both from performance and stability perspectives. We gauged the stability of the minimodules in accelerated degradation experiments, according to the IEC standards. These harsh tests are identical to those used to evaluate the stability of commercial c-Si PV and are meant to stress the solar cell and the module packaging simultaneously. These tests are part of a larger certification protocol to assess the mechanical and performance stability of commercial solar panels. By themselves, they do not provide a direct indication of what is the long term (>25 years) stability of the device during field operation but are fundamental to understand the main failure mechanisms both in the device and in the packaging. We subjected our minimodules to 50 thermal cycles (−40 to 85 °C) and 1000 hours of damp heat (DH, *i.e.* 85 °C at 85% relative humidity (RH), in dark). Remarkably, both encapsulants passed the thermal cycling (TC) test, which is among the first time for perovskite/silicon tandems. Finally, to better understand how the vacuum-laminated TPU and TPO-based samples perform under thermal cycling, thermomechanical analysis was performed.

Results and discussion

Fig. 1A shows the layer diagram constituting the perovskite/silicon tandem solar cell. Fig. 1B shows its scanning electron microscopy (SEM) cross-section, highlighting with colors the perovskite (blue) and the silicon (red) sub-cells and the textured silicon surface, featuring a levelized perovskite film due to the employed solution processing for the perovskite top cell. Fig. 1C shows the schematic composition of the mini-module, while Fig. 1D shows a top-view picture. For illuminated current–voltage (*IV*) measurements, we applied a shadow mask on the front glass to define a device active area of 1 cm^2. We report in Fig. 2A the statistical distribution of the PV performances before and after encapsulation with TPU and TPO. Overall, the minimodules preserve the initial performances when laminated with TPO as an encapsulant. On the contrary, with TPU the minimodules show a significant reduction of the short circuit current density, J_{sc}. Here we note that the absolute PCE is higher for the TPU case because of some batch-to-batch variation of the tandems. Fig. 2B and C show the *J–V* curves of the champion devices prior to and after encapsulation, highlighting that the only marked difference in performance after

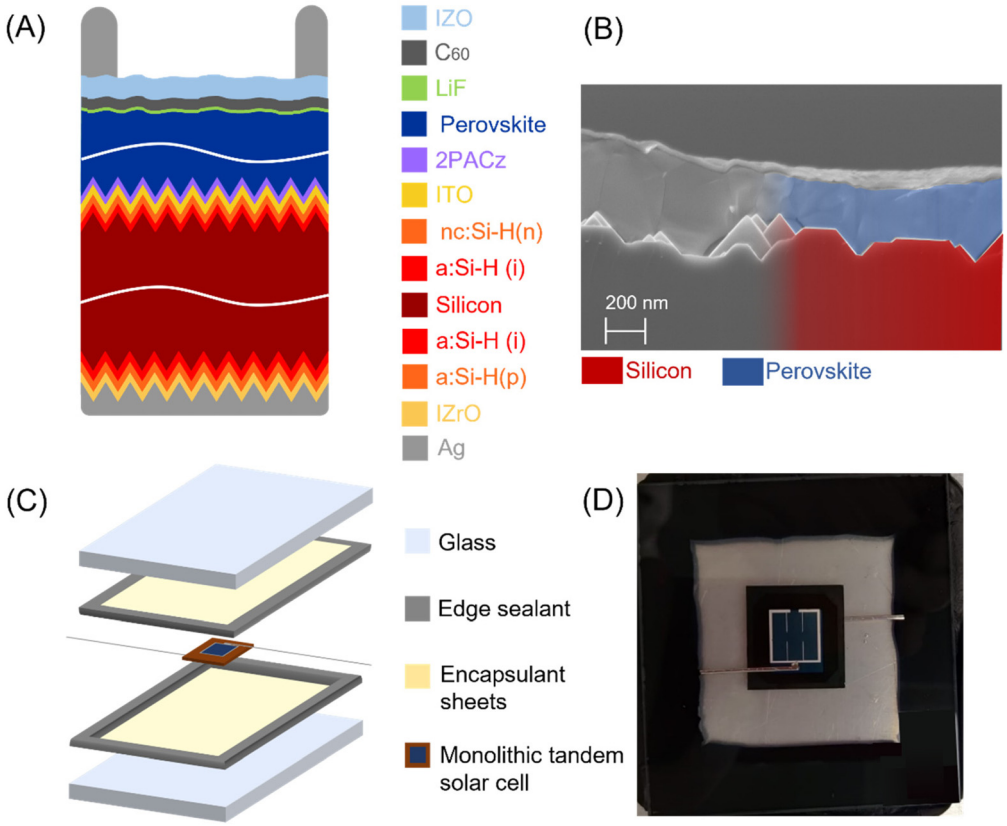

Fig. 1 (A) Schematic representation of the textured monolithic perovskite/silicon tandem solar cell. (B) Cross-sectional scanning electron microscopy image of the tandem solar cell. (C) Minimodule components representation. (D) Top view of the tandem minimodule.

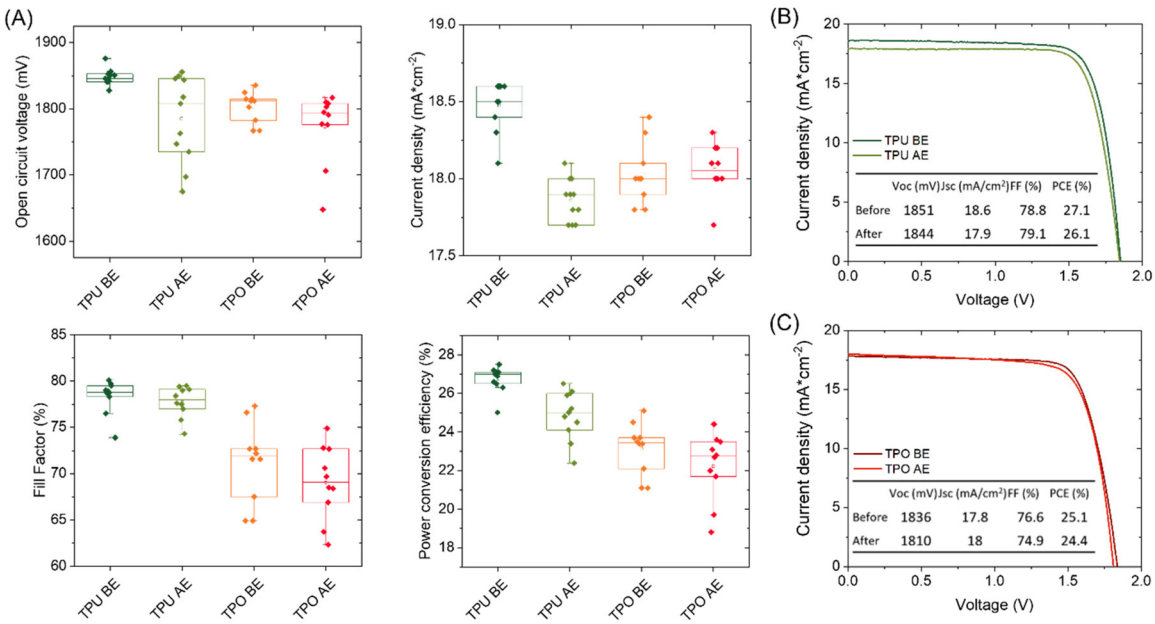

Fig. 2 *J*–*V* related parameters of monolithic perovskite/silicon tandem solar cell before and after encapsulation with TPU and TPO (A). Comparison between the *J*–*V* curves of the best devices before and after encapsulation with (B) TPU and (C) TPO.

the encapsulation process is given by a drop of J_{sc} when TPU is adopted.

Notably, the TPU-based material investigated here contains UV-blocking additives, resulting in a lower current generation in the perovskite top cell after encapsulation, thereby affecting the current matching of the tandem and, hence, its power output. To better understand the transmittance of the two encapsulants and their impact on performance, we optically characterized the two encapsulants, evaluating their UV-visible spectra obtained from the polymer sheets encapsulated between two glasses (Fig. 3C). TPU shows a UV cut-off at 400 nm, but a remarkable transparency in the near-IR. On the contrary, TPO shows very good transparency in the UV region, with a slightly higher absorption in the visible region. To understand the impact of the optical properties of the encapsulants we collected the external quantum efficiency (EQE) of the tandems before and after the encapsulation (Fig. 3D and E). Table 1 summarizes the sub-cells integrated currents, before and after the encapsulation. With TPU, we noted a significant reduction of the current generated by the perovskite sub-cell in the UV region, as expected from the absorption spectrum. Interestingly, both encapsulants enhance the current in the visible region. This is likely due to a better in-coupling of the light and a slight suppression of the reflection losses due to a reduction in the refractive index mismatch between the two media of the sunward-facing materials stack. We would like to highlight that the reduction in the integrated current is less pronounced compared with the average variation from the *JV* curves before and after encapsulation shown in Fig. 2A. With TPO, we noted a slight reduction of the current generated by the silicon sub-cell, which is likely due to a batch-to-batch variation and not created by the encapsulant.

Table 1 Sub-cells' integrated currents before and after encapsulation with TPU and TPO

	J_{sc} perovskite (mA cm^{-2})	J_{sc} silicon (mA cm^{-2})
Before TPU	17.70	18.65
After TPU	17.81	17.81
Before TPO	17.70	18.62
After TPO	18.54	17.90

Generally, during vacuum lamination different pressure steps at constant temperature are employed to guarantee a complete lamination and to avoid the formation of air bubbles between the different layers.[26–28] In particular, Fig. 3A shows the pressure profiles when the minimodules are encapsulated with the two different encapsulants. Following heating, to increase the plasticity of the encapsulant, the lamination starts with an air evacuation step, crucial to guarantee the extraction of any air trapped in the polymeric network.[6] Subsequently, the lamination system's membrane starts increasing the top pressure, thus pressing the minimodule top-to-bottom. The pressing step must be optimized with different pressures and pressing times, specific for each encapsulant. Finally, the vacuum is removed, and the sealed module is extracted from the laminator.

Optimization of the encapsulation process is crucial to minimize possible delamination at the device level. In particular, this harmful mechanism can in some instances be

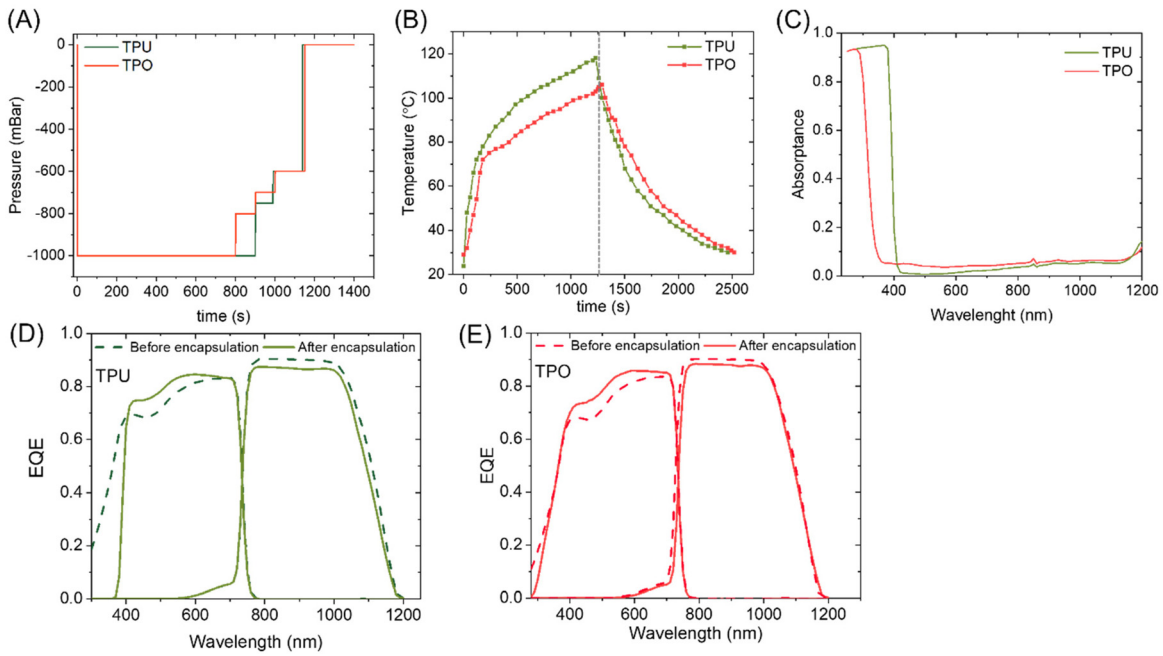

Fig. 3 (A) Pressure and (B) temperature profiles for the encapsulation process with the two encapsulants, the grey dotted line in the temperature profile indicates the end of the encapsulation process and the beginning of the minimodules' cooling down step. (C) UV-Visible characterization of the two encapsulants. (D) External quantum efficiency measures before and after encapsulation with TPU and (E) TPO.

observed at a macroscopic level (Fig. 4A) where the encapsulant peels off the perovskite cell's top contact, leading to a catastrophic failure of the device. Moreover, several studies indicated that the interface between the C_{60} electron transport layer (ETL) and SnO_x buffer layer is prone to delaminate.[6,16,29,30] The macroscopic delamination originates from the localized detachment of the buffer layer from the ETL surface, as evident in the cross-sectional SEM image (Fig. 4B), which can propagate to catastrophic failure or be confined to microscopic events, inducing a significant drop in the solar cell's overall performance.

To study this phenomenon, we performed adhesion experiments after lamination of the TPU on the tandem cell. In the adhesion experiments, we use peel testing of the encapsulants from the tandem surface to identify the weakest interface (ESI Fig. 1†). After initial tensioning of the encapsulants, we found an abrupt drop in the work of adhesion (WoA), which overlaps with the beginning of the macroscopic delamination. This confirms previous work which demonstrated that delamination at the C_{60}/SnO_x interface of the top contact in tandem solar cells is a critical issue to be addressed.[31] Whilst in most cases for both the TPO and TPU materials encapsulation was successful, we note that in some cases visible delamination was observed after lamination for cells encapsulated with TPO. This delamination occurred seemingly randomly, and we attribute it to defects within the tandem cells which are exacerbated during cooling of the encapsulant. This contrasts with TPU-based lamination, which showed almost zero delamination events, even after prolonged thermal stresses. We believe that the different thermomechanical properties of these two polymers are the reason for their specific differences in resilience against delamination.

To better understand the properties of the two encapsulants and gain insight into how they behave during vacuum-lamination and thermal cycling, thermomechanical analyzes were carried out. Polymer elastomers with low moduli, around 21 MPa, were originally selected as good encapsulation materials based on the requirement that they should not stress the solar cells during thermal cycling, as there is a large mismatch in thermal expansion coefficient between the inorganic solar cells and encapsulant.[32] This issue becomes even more critical for perovskite/silicon tandems for which delamination within the solar cell stack has already been highlighted.[31] The elastic modulus of the vacuum-laminated TPO and TPU used in this

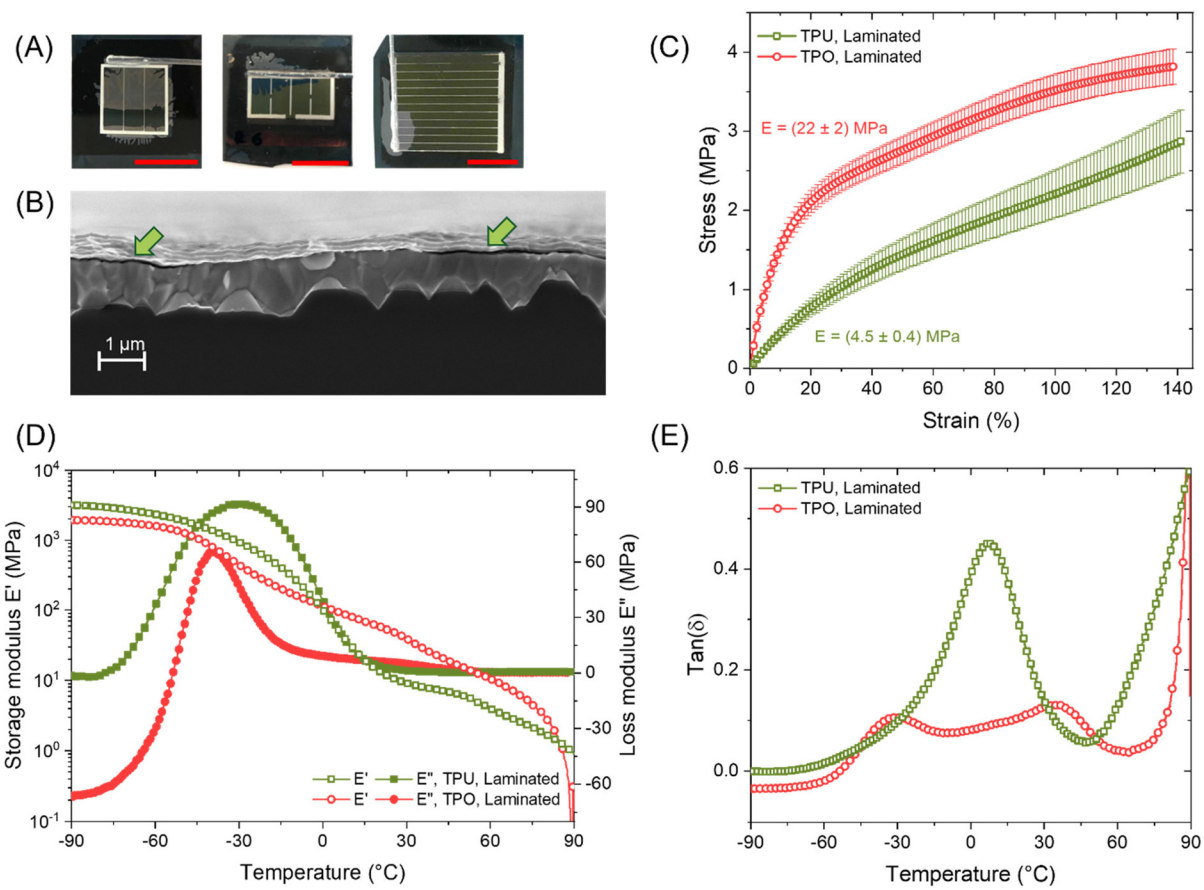

Fig. 4 (A) Macroscopic delamination observed on different tandem layouts with different sizes. Red bar: 1 cm. (B) Microscopic delamination observed *via* a cross-sectional scanning electron microscopy image of the tandem solar cell. For vacuum-laminated (cured) samples of TPU and TPO: (C) Stress–strain curves. (D) Storage and loss moduli as a function of temperature. (E) tan(δ) as a function of temperature.

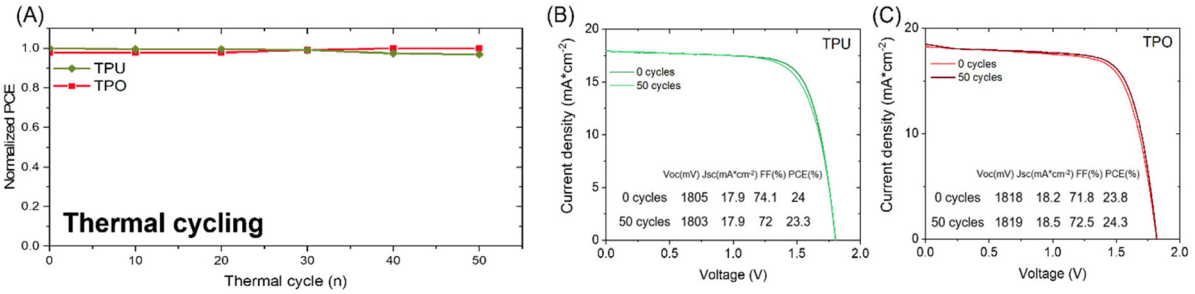

Fig. 5 (A) Power conversion efficiency trend during 50 cycles of TC test. (B) and (C) Comparison between the *J*–*V* curves before and after the TC test in the case of two minimodules encapsulated with TPU and TPO, respectively.

study were determined as 22 MPa and 4.5 MPa respectively. The stress–strain curves from which the elastic moduli were determined are shown in Fig. 4C.

The thermal properties of the two encapsulant materials were investigated using thermogravimetric analysis (TGA) and differential scanning calorimetry (DSC) and the resulting thermograms are shown in ESI Fig. 2 and 3.† Thermoplastic polyurethanes are block copolymers that combine hard and soft segments and their associated properties. The phase separation between these blocks can form rigid domains located in a rubbery matrix, and these domains can act as physical crosslinking points which account for the elastomeric behaviour of the amorphous TPU material. In contrast, TPO presents a flexible component, cross-linked with thermo-reversible crystalline domains, combining the properties of both rubbery and plastic materials.

To investigate how these two polymers dissipate energy within the encapsulated tandems during thermal cycling, dynamic mechanical analysis was carried out. The storage (E') and loss (E'') moduli describe the materials' viscoelastic behaviour as a function of temperature and are plotted in Fig. 4D. The E' of laminated TPU and TPO in the initial glassy state (at −90 °C) were higher than 10^3 Pa. In the applied temperature ramp of 2 °C min^{-1}, the E' *versus* temperature curves show a continuous drop of E' values, while E'' *versus* temperature curves show peak profiles, which are related to the molecular dissipative transitions allowed when the materials reach more flexible states. As also observed in the DSC, laminated TPU presents a broad temperature range related to the innumerous relaxation modes within the polymeric microstructure, including its glass transition. On the other hand, laminated TPO presents a narrower temperature range related to its glass transition, followed by melting (above 60 °C) of its crystalline domains (and reversible crosslinking sites), as observed in the DSC heating curves.

Finally, the tan(δ) (or loss factor), displayed in Fig. 4E, measures the overall energy dissipation of a material, and it is the ratio of the loss to the storage modulus. The tan(δ) values of the two encapsulants are plotted as a function of temperature in Fig. 4E. Laminated TPU presents higher tan(δ) values than laminated TPO, and therefore TPU has a higher energy dissipation capacity than TPO, especially in the relevant temperature range for module thermal cycling, more efficiently avoiding the microfracturing and delamination of the perovskite/silicon tandem devices. This is in line with our observations that delamination is more typically observed when encapsulating with TPO compared with TPU.

Lastly, we subjected our tandems encapsulated with TPU and TPO to the harsh IEC 61215 accelerated stability tests, in particular, 50 cycles of TC test (Fig. 5), in which in one cycle the temperature varies from +85 °C to −40 °C (over a period of 150 hours), and 1000 h of damp-heat (DH) testing (ESI Fig. 5†). Both the encapsulants passed the TC test confirming the possibility to adopt thermoplastic polymers even for relatively low-temperature encapsulations, despite thermomechanical analysis indicating that TPU could be better suited to minimizing the stress imposed on encapsulated tandem devices during thermal cycling.

Conclusions

We have shown the important role of the encapsulant in preserving the performance and stability of perovskite/silicon tandems. For stable devices, the right choice of encapsulant is strategic. With the exclusion of the widely adopted EVA, alternative polymeric encapsulants take the scene. Here, we compared the encapsulation of perovskite/silicon tandem minimodules using two thermoplastic polymers (TPU and TPO) that are in the spotlight for EVA's alternatives. Minimodules fabricated with both encapsulants were tested with accelerated stability tests: TC and DH, according to the IEC 61215 certifications and both configurations passed the thermal cycle test. Compared to TPO, TPU showed easier processing with negligible delamination events. This is in line with dynamic thermomechanical analysis of the two materials, from which TPU is shown to have higher tan(δ) values in the temperature range relevant for thermal cycling and therefore the ability to dissipate more energy within an encapsulated tandem, thereby protecting the device from stress. Utterly, this shows the importance of investigating perovskite/silicon tandem modules to further improve the stability of this technology.

Author contributions

Francesco Toniolo: conceptualization, data curation, analysis; Michele De Bastiani: conceptualization, data curation, analysis, writing original draft; Maxime Babics: conceptualization, data curation, analysis; Jiang Liu conceptualization, data curation, analysis; Ahmed Ali Said: conceptualization, data curation, analysis; Helen Bristow: conceptualization, data curation, analysis; Livia Loiola: mechanical and dynamic thermomechanical analysis of polymeric materials, conceptualization, data curation; Lujia Xu: data curation, analysis; Erkan Aydin: data curation, analysis; Thomas Allen: data curation, analysis; Moreno Meneghetti: funding acquisition, supervision, writing review; Suzana P. Nunes: funding acquisition, supervision, writing review. Stefaan De Wolf: funding acquisition, supervision, writing original draft, writing review.

Conflicts of interest

There are no conflicts to declare.

Acknowledgements

This work was supported by the King Abdullah University of Science and Technology (KAUST) Office of Sponsored Research (OSR) under award no. OSR-CARF/CCF-3079, OSR-CRG2019-4093, OSR-CRG2020-4350, IED OSR-2019-4208, IED OSR-2019-4580, and REI/1/4833-01-01.

References

1 S. De Wolf, *et al.*, Organometallic halide perovskites: Sharp optical absorption edge and its relation to photovoltaic performance, *J. Phys. Chem. Lett.*, 2014, **5**, 1035–1039.
2 J. M. Ball and A. Petrozza, Defects in perovskite-halides and their effects in solar cells, *Nat. Energy*, 2016, **1**, 1–13.
3 G. E. Eperon, *et al.*, Formamidinium lead trihalide: a broadly tunable perovskite for efficient planar heterojunction solar cells, *Energy Environ. Sci.*, 2014, **7**, 982–988.
4 M. Kim, *et al.*, Conformal quantum dot-SnO2 layers as electron transporters for efficient perovskite solar cells, *Science*, 2022, **375**, 302–306.
5 . Best Research-Cell Efficiency Chart | Photovoltaic Research | NREL. **https://www.nrel.gov/pv/cell-efficiency.html**.
6 M. De Bastiani, *et al.*, All Set for Efficient and Reliable Perovskite/Silicon Tandem Photovoltaic Modules?, *Sol. RRL*, 2022, **6**, 2100493.
7 P. Holzhey and M. Saliba, A full overview of international standards assessing the long-term stability of perovskite solar cells, *J. Mater. Chem. A*, 2018, **6**, 21794–21808.
8 N. J. Jeon, *et al.*, Compositional engineering of perovskite materials for high-performance solar cells, *Nature*, 2015, **517**, 476–480.
9 E. H. Anaraki, *et al.*, Highly efficient and stable planar perovskite solar cells by solution-processed tin oxide, *Energy Environ. Sci.*, 2016, **9**, 3128–3134.
10 R. Azmi, *et al.*, Damp heat-stable perovskite solar cells with tailored-dimensionality 2D/3D heterojunctions, *Science*, 2022, **376**, 73–77.
11 L. Shi, *et al.*, Gas chromatography-mass spectrometry analyses of encapsulated stable perovskite solar cells, *Science*, 2020, **368**(6497), eaba2412.
12 E. Ugur, *et al.*, How Humidity and Light Exposure Change the Photophysics of Metal Halide Perovskite Solar Cells, *Sol. RRL*, 2020, **4**, 2000382.
13 J. Sung Yun, *et al.*, Humidity-Induced Degradation via Grain Boundaries of HC(NH2)2PbI3 Planar Perovskite Solar Cells, *Adv. Funct. Mater.*, 2018, **28**, 1705363.
14 Q. Wang, *et al.*, Scaling behavior of moisture-induced grain degradation in polycrystalline hybrid perovskite thin films, *Energy Environ. Sci.*, 2017, **10**, 516–522.
15 Q. Dong, *et al.*, Encapsulation of Perovskite Solar Cells for High Humidity Conditions, *ChemSusChem*, 2016, **9**, 2597–2603.
16 R. Cheacharoen, *et al.*, Design and understanding of encapsulated perovskite solar cells to withstand temperature cycling, *Energy Environ. Sci.*, 2018, **11**, 144–150.
17 M. de Bastiani, *et al.*, Toward Stable Monolithic Perovskite/Silicon Tandem Photovoltaics: A Six-Month Outdoor Performance Study in a Hot and Humid Climate, *ACS Energy Lett.*, 2021, **6**, 2944–2951.
18 M. Babics, *et al.*, Unleashing the Full Power of Perovskite/Silicon Tandem Modules with Solar Trackers, *ACS Energy Lett.*, 2022, 1604–1610, DOI: **10.1021/ACSENERGYLETT.2C00442**.
19 L. C. Olsen, S. N. Kundu, C. C. Bonham and M. Gross, *Barrier Coatings for CTGSS And CDTE Cells*, 2005.
20 L. Xu, Efficiency loss of thin film Cu(InxGa1-x)Se(S) solar panels by lamination process, *J. Appl. Phys.*, 2017, **121**, 15.
21 Z. Fu, *et al.*, Encapsulation of Printable Mesoscopic Perovskite Solar Cells Enables High Temperature and Long-Term Outdoor Stability, *Adv. Funct. Mater.*, 2019, **29**, 1809129.
22 M. I. Asghar, J. Zhang, H. Wang and P. D. Lund, Device stability of perovskite solar cells – A review, *Renewable Sustainable Energy Rev.*, 2017, **77**, 131–146.
23 J. Bisquert and E. J. Juarez-Perez, The Causes of Degradation of Perovskite Solar Cells, *J. Phys. Chem. Lett.*, 2019, **10**, 5889–5891.
24 M. D. Kempe, *et al.*, Acetic acid production and glass transition concerns with ethylene-vinyl acetate used in photovoltaic devices, *Sol. Energy Mater. Sol. Cells*, 2007, **91**, 315–329.
25 R. Cheacharoen, *et al.*, Encapsulating perovskite solar cells to withstand damp heat and thermal cycling, *Sustainable Energy Fuels*, 2018, **2**, 2398–2406.
26 R. F. M. Lange, Y. Luo, R. Polo and J. Zahnd, The lamination of (multi)crystalline and thin film based photovoltaic modules, *Prog. Photovoltaics*, 2011, **19**, 127–133.

27 A. El Amrani, A. Mahrane, F. Y. Moussa and Y. Boukennous, Solar Module Fabrication, *Int. J. Photoenergy*, 2007, **2007**, 027610.
28 S. Pescetelli, *et al.*, Integration of two-dimensional materials-based perovskite solar panels into a stand-alone solar farm, *Nat. Energy*, 2022, **7**, 597–607.
29 N. Rolston, *et al.*, Engineering Stress in Perovskite Solar Cells to Improve Stability, *Adv. Energy Mater.*, 2018, **8**, 1802139.
30 I. T. Sachs-Quintana, *et al.*, Electron Barrier Formation at the Organic-Back Contact Interface is the First Step in Thermal Degradation of Polymer Solar Cells, *Adv. Funct. Mater.*, 2014, **24**, 3978–3985.
31 M. De Bastiani, *et al.*, Mechanical Reliability of Fullerene/Tin Oxide Interfaces in Monolithic Perovskite/Silicon Tandem Cells, *ACS Energy Lett.*, 2022, **7**, 827–833.
32 E. F. Cuddihy, Flat-plate solar array project, Volume 7: Module encapsulation, No. NASA-CR-180665, 1986.